ATLAS NOTE

ATLAS-CONF-2012-005

February 14, 2012

Search for supersymmetry with jets, missing transverse momentum and one or more τ leptons in proton-proton collisions at $\sqrt{s} = 7$ TeV with the ATLAS detector

The ATLAS Collaboration

Abstract

A search for production of supersymmetric particles in final states containing jets, missing transverse momentum, and one or more tau leptons is presented. The data were recorded by the ATLAS experiment in $\sqrt{s} = 7$ TeV proton-proton collisions at the Large Hadron Collider. No excess above the Standard Model background expectation was observed in 2.05 fb^{-1} of data. The results are interpreted in the context of GMSB models with $M_{\rm mess} = 250$ TeV, $N_5 = 3$, $\mu > 0$, and $C_{\rm grav} = 1$, excluding the production of supersymmetric particles up to $\Lambda = 40$ TeV for $\tan\beta > 15$ at 95% C.L.

1 Introduction

Supersymmetry (SUSY) is an attractive theory to remedy various shortcomings of the Standard Model (SM), such as the hierarchy problem, the lack of a dark matter candidate and the non-unification of the gauge couplings [1, 2, 3, 4, 5, 6, 7, 8, 9]. To achieve this, the SUSY masses must be near the weak scale, and therefore, if weak-scale SUSY is realized in nature, there are excellent chances to discover it at the LHC. In certain SUSY models, large mixing between left and right scalar fermions implies that the lightest partners of the SM fermions belong to the third generation, thus leading to a large production rate of τ leptons from decays of gauginos and $\tilde{\tau}$ leptons in SUSY cascade decays. For example, in the context of Gauge Mediated SUSY Breaking (GMSB) the lighter of the two scalar $\tilde{\tau}$ leptons is the next-to-lightest supersymmetric particle (NLSP) for a large part of the parameter space. In GMSB, $\tilde{\tau}$ leptons produced in SUSY cascade decays subsequently decay to a τ lepton and a stable light gravitino which creates missing transverse momentum in the detector.

In this note, a search for supersymmetry in final states with one or more τ leptons, missing transverse momentum and jets is presented. The search was carried out with the ATLAS detector at the LHC and the results are interpreted within the GMSB model. Previous experiments have placed constraints on $\tilde{\tau}$ and $\tilde{e}$ masses and on more generic GMSB topologies [10, 11].

2 ATLAS detector

The ATLAS detector [12] is a multipurpose particle physics apparatus with a forward-backward symmetric cylindrical geometry and nearly 4π coverage in solid angle [1]. The inner tracking detector consists of a silicon pixel detector, a silicon microstrip detector, and a transition radiation tracker. The inner detector is surrounded by a thin superconducting solenoid providing a 2 T magnetic field and by high-granularity liquid-argon sampling calorimeters. An iron-scintillator tile calorimeter provides hadronic coverage in the central rapidity range. A muon spectrometer surrounds the calorimeters and consists of three large superconducting toroids and a system of precision tracking chambers.

3 Data and simulated samples

The analysis is based on data collected by the ATLAS detector in proton-proton collisions at a center-of-mass energy of 7 TeV between March and August 2011. Application of beam, detector, and data-quality requirements resulted in an integrated luminosity of (2.05 ± 0.08) fb^{-1} [13]. The data were collected using triggers based on one high-p_{T} jet and large missing transverse momentum with thresholds of 75 GeV and 45 GeV, respectively, measured at the electromagnetic scale.

In GMSB models, the breaking of SUSY is mediated through flavor-blind SM gauge interactions via messenger fields at a mass scale, M_{mess}, which is small compared to the Planck mass. In addition to M_{mess}, the free parameters in GMSB models are the scale of the SUSY breaking, Λ, the number of messenger fields, N_5, the sign of the Higgsino mixing parameter, $sign(\mu)$, the scale factor for the gravitino mass, C_{grav}, and the ratio of the vacuum expectation values of the two Higgs doublets, $\tan\beta$. In this analysis, GMSB models are studied in the $\Lambda - \tan\beta$ plane for fixed $M_{\mathrm{mess}} = 250$ TeV, $N_5 = 3$, $sign(\mu) = +1$ and $C_{\mathrm{grav}} = 1$. The chosen set of parameter values restricts the analysis to specific final states relevant for the search with τ leptons and to promptly decaying NLSPs. For $N_5 \geq 2$ and large $\tan\beta$, for example, the lightest stau lepton, $\tilde{\tau}_1$, is the NLSP.

[1] ATLAS uses a right-handed coordinate system with its origin at the nominal interaction point in the center of the detector and the z-axis coinciding with the axis of the beam pipe. The x-axis points from the interaction point to the center of the LHC ring, and the y-axis points upward. Cylindrical coordinates (r, ϕ) are used in the transverse plane, ϕ being the azimuthal angle around the beam pipe. The pseudorapidity is defined in terms of the polar angle θ as $\eta = -\ln\tan(\theta/2)$.

Samples of simulated GMSB events are generated with the Herwig++ [14] generator for ten values of Λ in the range $10 \leq \Lambda \leq 85$ TeV and ten values of $\tan\beta$ in the range $2 \leq \tan\beta \leq 45$, with the SUSY mass spectra generated using ISAJET 7.80 [15]. The MRST2007 LO* [16] parton distribution functions (PDFs) are used. The production cross sections are calculated with PROSPINO [17, 18, 19, 20] to next-to-leading order in QCD using the next-to-leading order CTEQ6.6 [21] PDF set. The two samples with $\Lambda = 30$ (40) TeV and $\tan\beta = 20$ (30) with cross sections of 1.95 (0.41) pb are used as representative points for the optimization of the event selection.

The dominant background processes in this search are production of W and Z bosons in association with jets (W + jets, Z + jets), top-pair ($t\bar{t}$) and single-top production. W + jets and Z + jets production is simulated with the ALPGEN [22] generator, using the CTEQ6L1 [23] PDF set. The $t\bar{t}$ and single-top production processes are generated with MC@NLO [24] and the CTEQ6.6 [21] PDF set. For di-boson production, HERWIG [25] and MC@NLO are used. The parton shower and hadronization are simulated with HERWIG and the underlying event with JIMMY [26]. The programs TAUOLA [27, 28] and PHOTOS [29] are used to model the decays of τ leptons and the radiation of photons, respectively. The production of multijet events is simulated with PYTHIA [30]. All simulated samples are processed through a full simulation of the ATLAS detector based on Geant4 [31, 32]. To match the pile-up (overlap of several interactions in the same bunch crossing) observed in the data, minimum-bias events [33, 34] are overlaid to the generated signal and background events, and the resulting events are reweighted so that the distribution of the number of interactions per bunch crossing agrees with the data.

4 Object reconstruction

Jet candidates are reconstructed with the anti-k_t clustering algorithm [35] with radius parameter $R = 0.4$. The inputs to this algorithm are clusters of calorimeter cells seeded by cells with energy significantly above the measured noise. Jets are constructed by performing a four-vector sum over these clusters, treating each cluster as a four-vector with zero mass. Jets are corrected for calorimeter non-compensation, upstream material, and other effects using p_{T}- and η-dependent correction factors obtained from Monte Carlo and validated with extensive test-beam and collision-data studies [36]. Only jets with $p_{\mathrm{T}} > 30$ GeV and $|\eta| < 2.8$ are considered.

The electron and muon identification criteria are identical to those in Ref. [37]. Electrons and muons are only considered if they satisfy $p_{\mathrm{T}} > 20$ GeV and $\Delta R > 0.4$ with respect to the nearest identified jet, where the distance $\Delta R = \sqrt{(\Delta\eta)^2 + (\Delta\phi)^2}$.

The magnitude of the missing transverse momentum, $E_{\mathrm{T}}^{\mathrm{miss}}$, is computed from the vector sum of the transverse momenta of all identified electrons and muons, all jets, and remaining clusters of calorimeter cells with $|\eta| < 4.5$ [38].

Tau leptons are identified through their hadronic decay channels. Tau candidates are reconstructed from jet candidates with $p_{\mathrm{T}} > 10$ GeV and are distinguished from quark- or gluon-initiated jets using a boosted decision tree (BDT) based on eleven discriminating shower-shape and tracking variables [39]. Electrons are further rejected using transition radiation and calorimetry information. τ-specific, p_{T}- and η-dependent energy calibration factors are also applied. Tau candidates are required to satisfy $p_{\mathrm{T}}^{\tau} > 20$ GeV and $|\eta| < 2.5$ and to have one or three associated reconstructed tracks (prongs) with total charge ± 1. Tau candidates are required to satisfy a p_{T}-dependent selection criterion on the BDT output [39], chosen to give $\sim 30\%$ ($\sim 50\%$) signal efficiency for one-prong (three-prong) τ candidates as estimated in $Z(\rightarrow \tau\tau)$ + jets events. The BDT selection has a corresponding background acceptance of $\sim 0.5\%$ ($\sim 3\%$), estimated in dijet events, and the different selection criteria reflect different abundances of one- and three-prong jets in background samples.

During a part of the data-taking period, an electronics failure in the liquid-argon calorimeter created a dead region in the detector, corresponding to approximately 1.4×0.2 rad in $\Delta\eta \times \Delta\phi$. Electron and

τ candidates falling in this region are discarded. A correction is made to the jet energy using energy depositions in cells neighboring the dead region; events having at least one jet in this region for which the corrected energy is above 30 GeV are discarded, resulting in a loss of $\sim 6\%$ of the data sample.

5 Event selection

Events are required to have a reconstructed primary vertex with at least five associated tracks. Events are rejected if they contain identified electrons or muons or if any jet or τ candidate is consistent with arising from detector noise or non-collision background [40]. Events are required to contain one or more identified τ candidate, at least two jets, one with $p_{\mathrm{T}} > 30$ GeV and another with $p_{\mathrm{T}} > 130$ GeV, and missing transverse momentum $E_{\mathrm{T}}^{\mathrm{miss}} > 130$ GeV. The latter two requirements ensure that the trigger efficiency is above 98% in both data and simulation.

The two leading jets are required to be separated in azimuth from the direction of the missing transverse momentum by more than 0.3 radians. This requirement reduces multijet events which typically have instrumental missing transverse momentum aligned with the leading jets. Multijet events are further suppressed by requiring $E_{\mathrm{T}}^{\mathrm{miss}}/m_{\mathrm{eff}} > 0.25$, where the effective mass, m_{eff}, is defined as the scalar sum of $E_{\mathrm{T}}^{\mathrm{miss}}$, the p_{T} of the two leading jets, and the p_{T}^{τ} of the leading τ candidate.

Events are required to have a transverse mass, m_{T}, above 110 GeV. The transverse mass is defined as $m_{\mathrm{T}} = \sqrt{m_{\tau}^2 + 2p_{\mathrm{T}}^{\tau}E_{\mathrm{T}}^{\mathrm{miss}}\left(1 - \cos\Delta\phi(p_{\mathrm{T}}^{\tau}, E_{\mathrm{T}}^{\mathrm{miss}})\right)}$, where $\Delta\phi(p_{\mathrm{T}}^{\tau}, E_{\mathrm{T}}^{\mathrm{miss}})$ is the azimuthal distance between the τ and the direction of the missing transverse momentum. This requirement suppresses backgrounds due to W + jets and top quark production. The remaining SM backgrounds are further suppressed by requiring $m_{\mathrm{eff}} > 600$ GeV. This selection defines the signal region for the analysis.

6 Background estimation

Background processes are divided into three classes which are estimated separately: events with real τ leptons from $t \to b\tau\nu$ decays (both top quark pair and single top production) and $W(\to \tau\nu)$ + jets events; events with fake τ candidates in top, W + jets, and Z + jets events; and events with fake τ candidates in multijet events. The two fake τ classes are treated separately to account for differences in τ misidentification probabilities due to different event topologies and jet composition.

Events with real τ leptons are estimated in a control region defined by replacing the nominal transverse mass selection with $m_{\mathrm{T}} < 70$ GeV. This control region is expected to contain more than 90% events with real τ leptons from top quark and W decays, with the remaining small backgrounds estimated from simulation. Within this region, top quark and W + jets yields are estimated with a maximum-likelihood fit to a BDT built from four variables: the number of b-quark jets, the total jet multiplicity, the transverse momentum of the second leading jet and the transverse thrust T of the event, defined as $T = \max_{|\vec{n}|=1}\{\sum_i \vec{n}\cdot\vec{p}_{\mathrm{T},i}/|\sum_i \vec{p}_{\mathrm{T},i}|\}$, where i runs over the missing transverse momentum and all jets with transverse momentum vectors $\vec{p}_{\mathrm{T},i}$ and the transverse thrust axis is given by the unit vector $\vec{n}$ for which the maximum is attained. Top quark events have more reconstructed b-quark jets, a higher jet multiplicity, higher jet momenta, and tend to be more spherical than W + jets events. Jets containing b quarks are identified with about 60% efficiency using secondary vertex reconstruction and 3-dimensional impact parameters of tracks associated with the jet [41].

For the estimation of backgrounds due to fake τ candidates in top quark, W + jets, and Z + jets events, a second control sample is defined by selecting events that satisfy either $70 < m_{\mathrm{T}} < 110$ GeV or $m_{\mathrm{eff}} < 600$ GeV. Multijet events are expected to make up less than 3% of this sample and are estimated from simulation. Within this control region, true τ backgrounds are subtracted using estimates derived from the true-τ dominated control region.

Backgrounds due to both true and fake τ leptons are extrapolated from the two control regions to the signal region using Monte Carlo simulations.

Backgrounds due to multijet events are estimated in a third control region in which either one of the two leading jets is aligned in azimuth with the missing transverse momentum or $E_{\mathrm{T}}^{\mathrm{miss}}/m_{\mathrm{eff}} < 0.25$. Within this sample, the probability for jets (which contain very few real τ leptons) to satisfy the τ selection criteria is estimated by applying the selection to randomly selected jet candidates. This probability is then used to extrapolate the multijet background prediction into the signal region. It is found that the multijet background makes up only a few percent of the total SM background in the signal region.

Possible contamination from SUSY signals has been considered in all three background-estimation control regions and is found to have a negligible effect on the results presented below.

7 Systematic uncertainties

Dominant systematic uncertainties on the estimated background yields are due to uncertainties in the jet energy scale (3–8%) [42], jet energy resolution (6–13%) [43], τ energy scale (2–10%) [39], statistical uncertainties in the data control regions (5–15%), and Monte Carlo uncertainties related to the extrapolation from the control regions to the signal region (10–20%). This last term includes statistical uncertainties in the simulation, variations in the assumed background composition, and Monte Carlo generator uncertainties (estimated by varying the shower matching, factorization and renormalization scales, α_S, and initial-state and final-state radiation). Additional uncertainties on W + jets and top quark backgrounds are estimated by varying the assumed b-quark identification efficiency within measured uncertainties (4–11%) [41]. Uncertainties on multijet background are estimated by studying correlations between m_{eff} and the azimuthal separation between the leading two jets and the missing transverse momentum. Additional systematic uncertainties, including those on the pile-up description in the simulation, are considered and found to be negligible.

In addition to the sources described above, systematic uncertainties on the SUSY signal cross section are estimated by varying the factorization and renormalization scales in PROSPINO up and down by a factor of two, by considering variations in α_S and by varying the proton PDFs within their set of uncertainties. These theoretical uncertainties total typically 8–12% across the relevant region of parameter space. Uncertainties are calculated separately for individual SUSY production processes.

8 Results

Figure 1 shows the distributions of $E_{\mathrm{T}}^{\mathrm{miss}}$, p_{T}^{τ}, and m_{eff} for data with all selection requirements applied except for that on m_{eff}, along with the corresponding estimated backgrounds. The numbers of expected SM background events and the observed number of events after the m_{eff} requirement are shown in Table 1. The data agree with the background expectation.

Based on these results, limits are placed on contributions beyond the SM. A model-independent limit on the visible cross section, defined as the product of production cross section, branching fraction to at least one τ lepton, acceptance, and efficiency, of 4.0 fb is derived at 95% confidence level (C.L.). Figure 2 shows an interpretation of the result as a 95% C.L. exclusion limit in the $M_{\mathrm{mess}} = 250$ TeV, $N_5 = 3$, $\mu > 0$, $C_{\mathrm{grav}} = 1$ slice of the GMSB model. The figure also shows the variation of the expected limit in response to $\pm 1\sigma$ fluctuations in the expected SM background and the SUSY cross sections. The excluded regions are calculated using a profile likelihood method with systematic uncertainties modeled as varying Gaussian-distributed nuisance parameters [44, 45]. The resulting limit is compared with previous exclusion limits from searches for $\tilde{\tau}$ and $\tilde{e}$ production and GMSB topologies at LEP [10, 11]. The region of small Λ and large $\tan\beta$ is theoretically excluded since it leads to tachyonic states. In this

Table 1: Expected SM background event yields after the final requirement on m_{eff} and number of events observed in data. All systematic uncertainties are included here, and the uncertainty on Σ_{SM}, the sum of all SM backgrounds, takes correlations between the individual background uncertainties into account. The true-τ purities are 53% and 64% for the top and W + jets backgrounds, respectively, and negligible for the Z+jets and multijet backgrounds. The estimated event yield for a GMSB signal with $\Lambda = 40$ TeV, $\tan\beta = 30$ is 9.1 ± 1.7 events.

Top	W + jets	Z + jets	QCD	Σ_{SM}	Data
5.6 ± 1.4	4.7 ± 1.5	2.4 ± 0.7	0.5 ± 0.6	13.2 ± 4.2	11

model, the production of supersymmetric particles can be excluded up to $\Lambda = 30$ TeV independent of $\tan\beta$ and up to $\Lambda = 40$ TeV for $\tan\beta > 15$ at 95% C.L.

A direct comparison of the GMSB limit obtained in this analysis with the one from the recent results of the ATLAS SUSY search in final states with two or more τ leptons [46] is shown in Fig. 3.

9 Conclusions

In conclusion, this note presents a search for supersymmetry in final states containing jets, missing transverse momentum, and one or more τ leptons. No excess of events is seen beyond the expected Standard Model backgrounds in 2.05 fb^{-1} of data, and limits are placed in the context of GMSB models. The limits obtained extend the results from previous experiments.

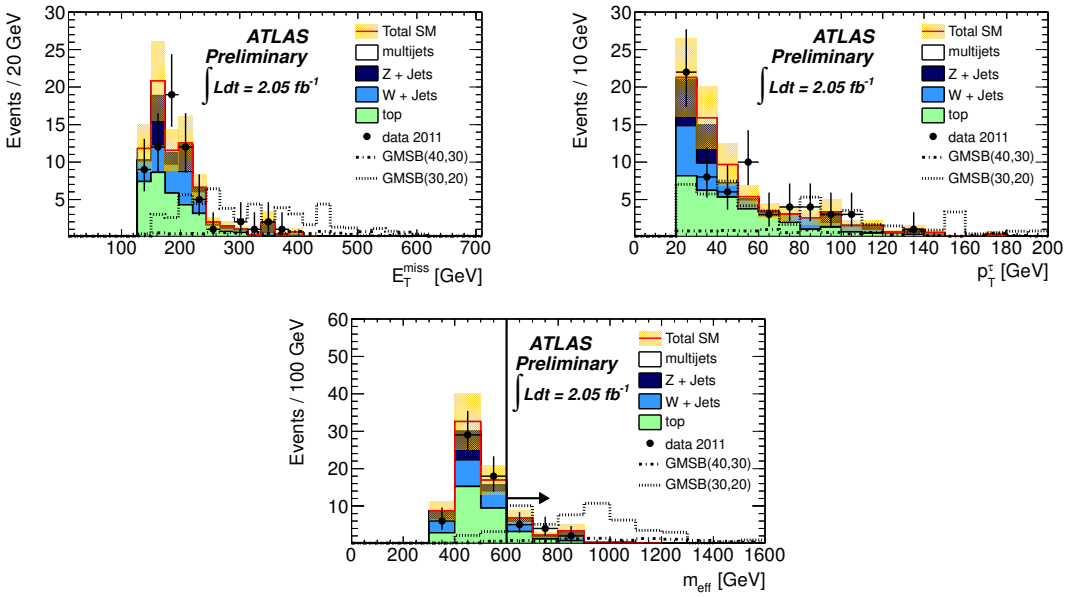

Figure 1: Distributions of $E_{\mathrm{T}}^{\mathrm{miss}}$, p_{T}^{τ}, and m_{eff} for data with all selection requirements except for that on m_{eff}, along with the corresponding estimated backgrounds. Backgrounds are taken from simulation and normalized with control regions in data. The error bands indicate the size of the total (statistical and systematic) uncertainty. The notation GMSB(40,30) stands for the GMSB model with $\Lambda = 40$ TeV and $\tan\beta = 30$.

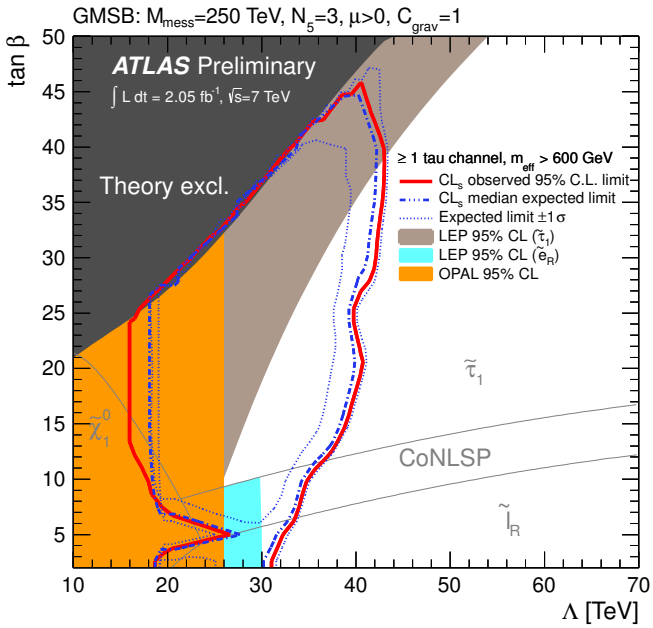

Figure 2: Expected and observed 95% C.L. exclusion limits from this analysis in the $M_{\mathrm{mess}} = 250$ TeV, $N_5 = 3$, $\mu > 0$, $C_{\mathrm{grav}} = 1$ slice of GMSB, together with the previous limits from LEP [10, 11]. The identity of the NLSP is indicated, with CoNLSP the region where the $\tilde{\tau}$ and $\tilde{\ell}$ are nearly degenerate.

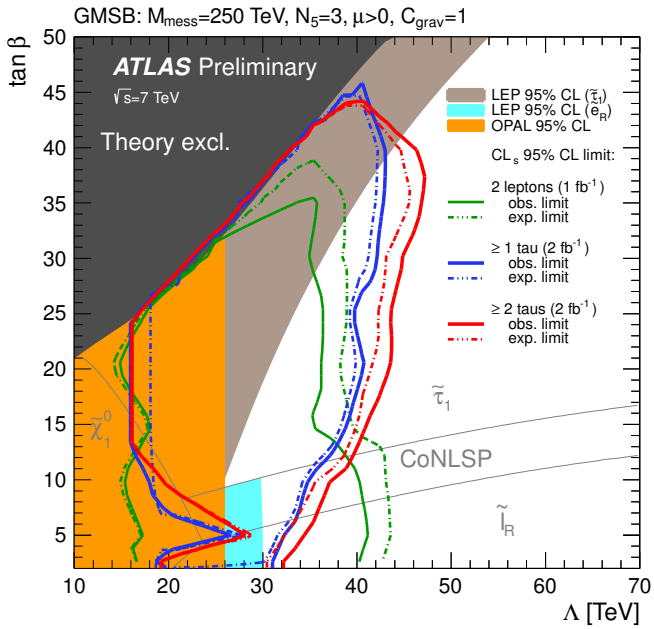

Figure 3: Expected and observed 95% C.L. exclusion limits in the $M_{\text{mess}} = 250$ TeV, $N_5 = 3$, $\mu > 0$, $C_{\text{grav}} = 1$ slice of GMSB. Shown are the limits from this ≥ 1 tau SUSY search, the ATLAS ≥ 2 taus SUSY search [46] and the ATLAS 2 leptons SUSY search [47], together with the limits from LEP [10, 11].

References

[1] P. Ramond, Phys. Rev. **D3** (1971) 2415–2418.

[2] Yu. A. Golfand and E. P. Likhtman, JETP Lett. **13** (1971) 323–326.

[3] A. Neveu and J. H. Schwarz, Nucl. Phys. **B31** (1971) 86–112.

[4] A. Neveuand J. H. Schwarz, Phys. Rev. **D4** (1971) 1109–1111.

[5] D. V. Volkov and V. P. Akulov, Phys. Lett. **B46** (1973) 109–110.

[6] J. Wess, and B. Zumino, Phys. Lett. **B49** (1974) 52.

[7] J. Wess and B. Zumino, Nucl. Phys. **B70** (1974) 39–50.

[8] P. Fayet, Phys. Lett. **B69** (1977) 489.

[9] G. R. Farrar and P. Fayet, Phys. Lett. **B76** (1978) 575–579.

[10] LEP SUSY WG/02-09.2 (2002), http://cern.ch/lepsusy.

[11] OPAL Collaboration, Eur. Phys. J. **C46** (2006) 307.

[12] ATLAS Collaboration, JINST **3** (2008) S08003.

[13] ATLAS Collaboration, ATLAS-CONF-2011-116.

[14] M. Bahr *et al.*, Eur. Phys. J. **C58** (2008) 639.

[15] F. Paige *et al.*,. arXiv:hep-ph/0312045, 2003.

[16] A. Sherstnev and R. S. Thorne, Eur. Phys. J. **C55** (2008) 553.

[17] W. Beenakker *et al.*, Nucl. Phys. **B492** (1997) 51.

[18] W. Beenakker *et al.*, Nucl. Phys. **B515** (1998) 3.

[19] W. Beenakker *et al.*, Phys. Rev. Lett. **83** (1999) 3780.

[20] T. Plehn, Czech. J. Phys. **55** (2005) B213.

[21] P. Nadolsky *et al.*, Phys. Rev. **D78** (2008) 013004.

[22] M. L. Mangano *et al.*, JHEP **07** (2003) 001.

[23] J. Pumplin *et al.*, JHEP **0207** (2002) 012.

[24] S. Frixione and B. R. Webber, JHEP **06** (2002) 029.

[25] G. Corcella *et al.*, JHEP **01** (2001) 010.

[26] J. M. Butterworth, J. R. Forshaw and M. H. Seymour, Z. Phys. **C72** (1996) 637.

[27] S. Jadach *et al.*, Comput. Phys. Commun. **76** (1993) 361.

[28] P. Golonka *et al.*, Comput. Phys. Commun. **174** (2006) 818.

[29] E. Barberio and Z. Was, Comput. Phys. Commun. **79** (1994) 291.

[30] T. Sjöstrand, S. Mrenna and P. Skands, JHEP **05** (2006) 026.

[31] Geant4 Collaboration, S. Agostinelli *et al.*, Nucl. Instrum. Meth. **A506** (2003) 250.

[32] ATLAS Collaboration, Eur. Phys. J. **C70** (2010) 823.

[33] ATLAS Collaboration, ATL-PHYS-PUB-2010-014.

[34] ATLAS Collboration, ATLAS-CONF-2010-031.

[35] M. Cacciari *et al.*, JHEP **04** (2008) 063.

[36] ATLAS Collaboration, ATLAS-CONF-2010-050 (2010); E. Abat *et al.*, Nucl. Instr. Meth. **A621** (2010) 134.

[37] ATLAS Collaboration, Phys. Rev. **D85** (2012) 012006.

[38] ATLAS Collaboration, Eur. Phys. J. **C72** (2012) 1844.

[39] ATLAS Collaboration, ATLAS-CONF-2011-152.

[40] ATLAS Collaboration, arXiv:1112.6426.

[41] ATLAS Collaboration, ATLAS-CONF-2011-102.

[42] ATLAS Collaboration, ATLAS-CONF-2011-032.

[43] ATLAS Collaboration, ATLAS-CONF-2011-054.

[44] G. Cowan *et al.*, Eur. Phys. J. **C71** (2011) 1554.

[45] A. Read, Journal of Physics G: Nucl. Part. Phys. **28** (2002) 2693.

[46] ATLAS Collboration, ATLAS-COM-CONF-2012-010.

[47] ATLAS Collboration, arXiv:1110.6189 [hep-ex], accepted by Phys. Lett. B.